# CPP

## Contributions to Plasma Physics

WILEY-VCH

REPRINT

# Atomic Ionization and Molecular Dissociation in a Hydrogen Gas within the Physical Picture

**A. Alastuey**[1] and **V. Ballenegger**[2*]

[1] Laboratoire de Physique, Ecole Normale Supérieure de Lyon, CNRS, 46 allée d'Italie, 69364 Lyon Cedex 07, France

[2] Institut UTINAM, Université de Franche-Comté, CNRS, 16 route de Gray, 25030 Besançon Cedex, France

We study a hydrogen gas at low densities within the physical picture. Recombination processes leading to the formation of atoms and molecules are properly taken into account *via* the well-known Ebeling function and a new four-body partition function. Our method provides a reliable equation of state which covers the plasma, atomic and molecular phases.

## 1 Introduction

We consider hydrogen in the low-density region of the phase diagram, where recombination processes lead to the formation of atoms or/and molecules. Contrarily to familiar chemical approaches which assume that those recombined entities are preformed objects with phenomenological internal partition functions and effective interactions, we describe hydrogen within the so-called physical picture in terms of a quantum plasma of point protons and electrons interacting *via* the Coulomb $1/r$ potential. Only the use of the physical picture can provide reliable equations of state (EOS) that reach the accuracy of experimental observations. Recent advances in helioseismology allow one for instance to probe the equation of state (EOS) of the solar matter —composed mainly of hydrogen — to an accuracy of better than $10^{-4}$ [1].

Atomic recombination or ionization was first considered in the framework of the physical picture by Ebeling [2]. More precisely, using Morita approach, Ebeling exactly computed the second virial coefficient (SVC) in the low-activity expansion, where atomic contributions are properly taken into account. The key quantity is some function $Q$, which can be expressed as an infinite sum over both bound and scattering states of the two-body Coulomb Hamiltonian. The finiteness of $Q$ is ensured by the substraction from the two-body Gibbs factor of non-integrable powers of the Coulomb potential, while the *a priori* divergent contributions of those powers are regularized thanks to screening by the ionized charges present in the medium. We stress that the screening mechanism that regularizes both the internal atomic partition function and the ionized charge-charge interactions in the SVC is treated in an exact way. Bound and scattering contributions are intrinsically mixed in function $Q$. The tight interplay between recombination and screening is such that these two effects cannot be fully disentangled. [1]

If Ebeling function $Q$ controls atomic corrections in the almost fully ionized regime at low densities and rather high temperatures, it was shown more recently that $Q$ is still a central quantity for the ionization equilibrium $H \rightleftarrows p + e$ in the partially ionized regime [3, 4] which can be attained by lowering the temperature along a low-density isochore. If temperature is further decreased beyond full atomic recombination, molecules form and become the most important chemical species. The main purpose of this paper is the description of that molecular recombination process within the physical picture. We show that the central quantity is now a cluster particle function $Z(2, 2)$ for two protons and two electrons, which can be viewed as a natural extension of Ebeling

---

* Corresponding author. E-mail: vincent.ballenegger@univ-fcomte.fr, Phone: +33 3 81 66 64 79, Fax: +33 3 81 66 64 75

[1] Accordingly, the extraction from $Q$ of an internal atomic partition function remains arbitrary. For instance the well-known Planck-Larkin-Brillouin formula is a possible choice. Nevertheless, as far as thermodynamic properties are concerned, only the full contribution of $Q$, including scattering states, plus the contributions from screening effects makes an unambiguous sense.

function $Q$. Our method, briefly sketched in Sec. 2 is based on the so-called Screened Cluster Representation for the density $\rho$ in terms of the chemical potential $\mu$ [5, 7]. That formalism allows us to deal with the interplay between screening and recombination into atoms, molecules, or any other species like ions $H^-$, $H_2^+$,..., in an exact way. Cluster partition function $Z(2,2)$ involves not only contributions from bound states of the molecule, but also from its dissociation products which can be associated with the various chemical equilibria $H_2 \rightleftarrows H + H$, $H_2 \rightleftarrows H_2^+ + e$, $H_2 \rightleftarrows H^- + p$, $H_2 \rightleftarrows H + p + e$, and $H_2 \rightleftarrows p + p + e + e$. As exposed in Sec. 2, an adequate choice of diagrams in the Screened Cluster Representation allows one to obtain an approximate function $\rho(\beta, \mu)$ which should be reliable in the considered low-density regime. Then, $\mu(\beta, \rho)$ is determined *via* a numerical inversion, and we compute the pressure along a low-density isochore that covers the fully ionized regime at high temperatures, the atomic phase at intermediate temperatures, and the molecular phase at lower temperatures (see Sec. 3). Our predictions are compared to numerical results of quantum Monte Carlo simulations [6] and to the tabulated OPAL EOS [8] derived using the ACTEX method [9]. In Sec. 4, we make some concluding comments.

## 2  Method

### 2.1  Recombination and screening



**Fig. 1**  A few SC diagrams in the Screened Cluster representation of the proton density. Bonds between particle clusters can be $\Phi$, $\frac{1}{2!}\Phi^2$ or $\frac{1}{3!}\Phi^3$.

The Screened Cluster (SC) representation is a resummed activity series expressed in terms of Mayer-like diagrams built with particle clusters and a screened effective potential $\Phi$ [5]. In Fig. 1, we show a few diagrams in the SC representation of the proton density $\rho_p = \rho_e = \rho$. The SC diagrams account, simultaneously and consistently, for

- **Recombination**: The statistical weights of particle clusters $Z(N_p, N_e)$ incorporate the contributions of bound states, because both quantum mechanics and Coulomb interactions are treated non-perturbatively.

- **Screening**: All large-distance contributions of diffusive states are finite, because effective interactions between particle clusters are screened.

When the density tends to zero, bare Coulomb Hamiltonians $H_{N_p, N_e} = -\sum_{i=1}^N \frac{\hbar^2}{2m_{\alpha_i}}\Delta_i + \frac{1}{2}\sum_{i \neq j}\frac{e_{\alpha_i}e_{\alpha_j}}{|\mathbf{r}_i - \mathbf{r}_j|}$ (where $\alpha_i = p$, e is the species of the $i$th particle, $e_{\alpha_i}$ its charge and $m_{\alpha_i}$ its mass) emerge at leading order in the statistical weights of particle clusters. The corresponding cluster partition functions $Z(N_p, N_e)$ reduce to finite truncated traces $\text{Tr}[\exp(-\beta H_{N_p,N_e} - \ldots)]$. The counter-terms substracted from Gibbs operator $\exp(-\beta H_{N_p, N_e})$ cancel out long-range divergences in the trace, while their own *a priori* divergent contributions remain finite thanks to the introduction of the screened potential $\Phi$. That exact construction, which gives rise in particular to diagrams made up of two or more clusters connected by bonds $\Phi$, $\frac{1}{2!}\Phi^2$ or $\frac{1}{3!}\Phi^3$, is systematically performed through the whole activity series [5]. Chemical species naturally emerge in cluster partition function $Z(N_p, N_e)$, which involves contributions from both bound and diffusive states.

The individual contributions of an atom H arise in diagram (b) shown in Fig. 1, and they are embedded in cluster partition function $Z(1,1)$. The contributions of the counter-terms associated to the truncation in $Z(1,1)$ are embodied in diagrams $p - \frac{1}{n!}\Phi^n - e$ with $n = 1, 2, 3$ (for instance diagram (c) when $n = 1$). Cluster partition function $Z(1,1)$ is in fact merely related to Ebeling function $Q(\beta)$. Similarly, hydrogen molecules $H_2$ emerge in diagram (d), and their contributions are embedded in cluster partition function $Z(2,2)$. All possible species resulting from molecular dissociation, namely p, e, H, $H_2^+$ and $H^-$ arise in the truncation of $\exp(-\beta H_{2,2})$. If cluster partition function $Z(2,2)$ contains contributions from all thermally excited states, the molecular ground-state contribution prevails in the zero-temperature limit.

Diagrams with bonds between the clusters describe screened interactions between the involved entities. Graph (f) accounts for instance for long-range van der Waals interactions between two H atoms, while graph (d) contains contributions linked to their short-range interactions.

### 2.2 Computation of the EOS at low densities

Along a low-density isochore, $\rho < 10^{-2}$ g/cc and for not too low temperatures $T > 10^3$ K, we have estimated the SC diagrams that provide the most important contributions to the density $\rho(\beta, z)$ where $\beta = 1/(kT)$ and $z = \exp(\beta\mu)$ is the fugacity [2]. It turns out that the relevant diagrams account for ideal contributions of ionized charges, atoms H, molecules $H_2$, plasma polarization and interactions between ionized charges and atoms H. All other diagrams, in particular those describing ions $H_2^+$ and $H^-$ or interactions between molecules can be neglected. This provides a quite reasonable approximation for $\rho(\beta, z)$, which takes a polynomial form in $\sqrt{z}$ with temperature-dependent coefficients. Most coefficients can be calculated analytically, while we used a simple approximation for $Z(2, 2)$ introduced in Ref. [13].

The pressure $P(\beta, \rho)$ is then computed as function of temperature and density by eliminating numerically the fugacity $z$ between equations $\rho = \rho(\beta, z)$ and $\beta P = z \partial/\partial z \rho(\beta, z)$. Notice that, by construction, the present calculation reproduces the first terms of the known exact asymptotic expansions, namely, on the one hand, the virial expansion [10, 11] valid in the almost fully ionized regime $\rho \to 0$ at $T$ fixed, and, on the other hand, the Scaled Low Temperature (SLT) expansion [4] valid in the Saha atomic regime $T \to 0$ with $\rho \sim e^{-|E_H|/(kT)}$.

## 3 Numerical results

### 3.1 At very low densities

At very low densities, molecules are very scarce along the full isochore, except at very low temperatures. Then, the pressure remains close to the predictions of Saha theory which describes an ideal mixture of ionized protons, ionized electrons and atoms in their groundstate. We plot in Fig. 2 the deviation $\beta(P - P_{\text{Saha}})/\rho$, on a logarithmic scale, along a very-low density isochore $\rho = 10^{-10}$ g/cc. That deviation agrees with the first two simple terms $P_1$ (plasma polarization) and $P_2$ (molecular recombination) of the fully analytical SLT expansion [4], apart at very low temperatures where the pressure approaches $\rho kT/2$ as expected.
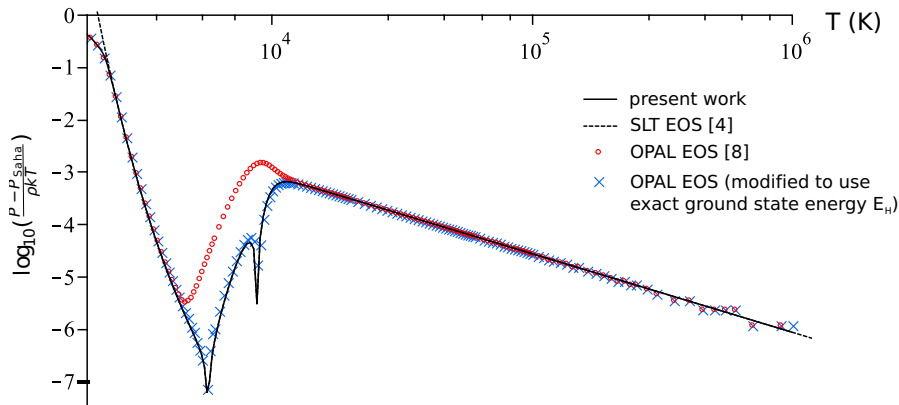


**Fig. 2** Log plot of deviations to the ideal Saha pressure along isochore $10^{-10}$ g/cc. Our predictions (solid line) are compared to the analytical SLT expansion (dashed line) and to the tabulated OPAL equation of state (circles). The crosses correspond to the OPAL EOS modified to account for the finite mass of the proton in the binding energy of the hydrogen atom, i.e. using $E_H = -me^4/(2\hbar^2) \simeq -13.5983$ eV instead of $E_H \simeq 1$ Ry $= -m_e e^4/(2\hbar^2) \simeq -13.65057$ eV. We corrected the OPAL values only at the level of the ideal terms: $P_{\text{OPAL, corr}} = P_{\text{OPAL}} + P_{\text{Saha}}[E_H] - P_{\text{Saha}}[1 \text{ Ry}]$.

### 3.2 At low and moderate densities

Now we consider an isochore at moderate densities, typically $\rho = 10^{-3}$ g/cc as shown in Fig. 3. At high temperatures, entropy wins and the gas is almost fully ionized, with pressure close to its ideal value $2\rho kT$. When temperature is lowered, energy enters into the game, so atomic recombination takes place and a first

---

[2] As rigorously proved in Ref. [12], only the mean chemical potential $\mu = (\mu_p + \mu_e)/2$ of protons and electrons is relevant in the thermodynamic limit, and it entirely determines the common particle density $\rho = \rho_p = \rho_e$.

plateau appears with pressure close to the ideal expression $\rho kT$ for a purely atomic gas. If we further lower the temperature, energy favors molecules since they are more stable than atoms. Then a second plateau appears with pressure close to the ideal value $\rho kT/2$ for a purely molecular gas.

The cross-over between the plasma and atomic phases is well captured by the thermal effects contained in function $Q$ which suitably corrects the predictions of Saha theory. In that region, the agreement between our calculations, the OPAL EOS [8] and Path Integral Monte Carlo (PIMC) simulations [6] is very good.

At temperatures lower than about $10^4$ K, the cross-over between the atomic and molecular phases is crucially controlled by function $Z(2,2)$. Our predictions deviate then somewhat from those of OPAL, while the numerical results of PIMC simulations have rather large uncertainties.
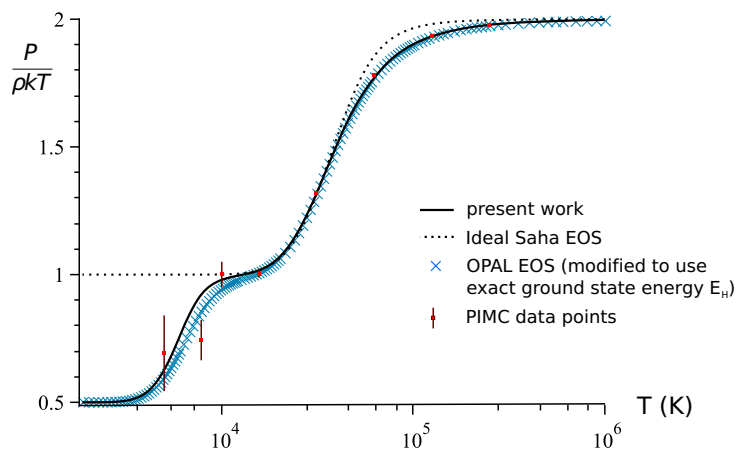


**Fig. 3** Pressure along isochore $10^{-3}$ g/cc. Crosses correspond to the OPAL EOS, as in Fig. 1. Numerical results of PIMC simulations [6] are also shown with their error bars.

Along the two considered isochores, the ionized charges remain always weakly coupled. The order of magnitude of the coupling constant $\Gamma$ can be estimated within the reasonable *ad-hoc* definition of the density of ionized charges as the sum of all SC diagrams (see Fig. 1) for which the root proton is the sole particle in the root cluster. For isochore $\rho = 10^{-3}$ g/cc, this provides $\Gamma_{\max} = 0.24$ which is reached when $T \simeq 28\,760$ K.

Notice that the order of magnitude of the cross-over temperatures between the successive ionized, atomic and molecular phases can be estimated from a simple criterion on the chemical potential, inspired by the atomic and molecular limit theorems at zero temperature [14, 15], which amounts to compare ideal densities of the corresponding chemical species in their groundstate. This provides $T \simeq 9000$ K (isochore $10^{-10}$ g/cc) and $T \simeq 40000$ K (isochore $10^{-3}$ g/cc) for atomic recombination, while $T \simeq 1700$ K (isochore $10^{-10}$ g/cc) and $T \simeq 3200$ K (isochore $10^{-3}$ g/cc) for molecular recombination. The comparison to our results displayed in Figs. 2 and 3 shows that the location of the cross-over between the plasma and the atomic gas is roughly recovered, while the discrepancy is larger for the transition to the molecular gas. This is not unexpected, since hydrogen molecules are obviously highly excited rotationally at the temperatures considered in Fig. 3.

## 4   Conclusions and perspectives

Within the physical picture, we have derived a reliable EOS which works rather well at low densities over a broad range of temperatures. Its key ingredients are Ebeling function $Q$ and cluster partition function $Z(2,2)$, which only depend on temperature $T$ and on the fundamental constants $\hbar, e, m_{\mathrm{p}}, m_{\mathrm{e}}$. Those functions are essential for describing properly the plasma-atomic and atomic-molecular cross-over regions.

Because of our poor knowledge of the exact spectrum of four-body Hamiltonian $H_{2,2}$, we had to use an approximate form for function $Z(2,2)$. An obvious improvement would be to better estimate that function, for instance through computationally exact numerical methods. Moreover, further studies of its analytical properties would be helpful for deriving simple modelizations of $Z(2,2)$. Such modelizations could then be used for constructing suitable internal molecular partition functions involved in chemical approaches applied to higher-density regimes.

## References

[1] W. Däppen, J. Phys. A: Math. Gen. **39**, 4441 (2006).

[2] W. Ebeling, Ann. Phys. Leipz. **19**, 104 (1967).

[3] W. Ebeling, M. Steinberg, J. Ortner, Eur. Phys. J. D **12**, 513-520 (2000).

[4] A. Alastuey, V. Ballenegger, F. Cornu and Ph.A. Martin, J. Stat. Phys. **130**, 1119-1176 (2008).

[5] A. Alastuey, V. Ballenegger, F. Cornu and Ph.A. Martin, J. Stat. Phys. **113**, 455-503 (2003).

[6] B. Militzer and D. M. Ceperley, Phys. Rev. E **63**, 066404 (2001).

[7] A. Alastuey and V. Ballenegger, J. Phys. A: Math. Theor. **42**, 214031 (2009).

[8] F.J. Rogers and A. Nayfonov, Astrophys. J. **576**, 1064-1074 (2002).

[9] F.J. Rogers, Phys. Review A **24**, 1531 (1981).

[10] W.D. Kraeft, D. Kremp, W. Ebeling, and G. Röpke, Quantum Statistics of Charged Particle Systems (Plenum Press, New York, 1986).

[11] A. Alastuey and A. Perez, Europhys. Lett. **20**, 19-24 (1992).

[12] E.H. Lieb and J. Lebowitz, Adv. Math. **9**, 316-398 (1972).

[13] A. Alastuey and V. Ballenegger, Contrib. Plasma Phys. **50**, 46-53 (2010).

[14] D.C. Brydges and Ph.A. Martin, J. Stat. Phys. **96**, 1163-1330 (1999).

[15] I. Iosilevskiy, Contrib. Plasma Phys. **49**, 713-717 (2009).